Development of a Solid Propellant Motor for High-Powered Model Rockets

Washington K. Kigani, Felix W. Gateru, Maureen W. Gichia, Valerian K. Nyerere, Jeff Mboya, Bernard Owiti, Shohei Aoki

***Abstract*—** High powered rocketry involves rockets with a total mass of more than 1,500 grams, a fuel mass of more than 125 grams and a propellant of more than 160 Newton-seconds of total impulse or a motor with an average thrust of 80 Newtons or more. Such rockets require high powered propulsion systems to be developed in order to achieve the required thrust and apogee. This paper highlights the design, simulation, and development of a high-powered propulsion system for the Nakuja-2 rocket with a desired apogee of 500 m. The design process was done with the goal to ensure the required thrust is achieved while ensuring safety. During the process, data was collected remotely by means of a developed data acquisition system and the developed solid propellant motor was able to generate an average thrust of 151.7 Newtons, getting the rocket to an apogee of 280 m.

***Keywords*—** Solid rocket propellant, Model rocket, Thrust

I. Introduction

Solid rocket motors were the first technological advances for both military and civilian propulsion systems [1]. Advances in the development of effective castable composite solid rocket fuel during World War II prompted intensified research on alternative formulations and the development of Potassium Perchlorate [2]. In order to minimise smoke and boost specific impulse, Aerojet substituted potassium perchlorate in various aeroplex propulsion systems with ammonium perchlorate in 1948 [3]. However, concerns with burning inconsistency forced Aerojet to switch to a polyurethane binding in 1953, while Rumbel and Henderson recommended aluminium fuel for improving performance in 1958 [2]. The use of aluminium powder in the solid rocket motor boosted thrust output but resulted in the development of liquid aluminium oxide particles and a two-phase flow in the chamber [2]-[4]. The above two-phase flow has an effect on pressure variations and causes slag deposition, nozzle degradation, and two-phase losses [4]-[6]. Nonetheless, because of the substantial energy output in the oxidation reaction to alumina, current solid rocket propulsion systems for aerospace purposes frequently employ nano particles as a fuel [7]-[9]. Although numerous high output options for aluminium substitution for high powered model rocket motors have been identified, the majority of them are far from being actually implemented in real model rocket applications [10]-[12]. As such, our rocket development team, the *Nakuja project*, seeks to build a high-power Potassium Nitrate-Sorbitol solid propellant rocket motor to propel the team's N-2 rocket to an apogee of 500 m. In this study, we conducted simulations to find out the appropriate Potassium Nitrate-Sorbitol mixtures to be cast in the solid rocket motor. We developed and cast the Potassium Nitrate-Sorbitol solid rocket motor based on the simulation parameters. We also made the nozzle to improve motor performance. Finally, we tested and evaluated the performance of the propellant. A comparison of models and actual data from testing is also presented in order to assess the effectiveness of the Potassium Nitrate-Sorbitol motor development process. The paper concludes with an assessment of the propellant's performance when integrated into the airframe of the N-2 rocket.

II. Design

Prior to the development of the solid propellant motor, designs were done in order to ensure that the fabricated propellant would meet all the outlined objectives without failure. Fusion 360 was used for modelling the casing, the bulkhead, and the nozzle.

The N-2 rocket was to be developed in order to incorporate a solid propellant rocket to get the rocket to an apogee of 500m. In order to remain aerodynamically stable in the operating environment and to be able to achieve the desired apogee, the N-2 rocket airframe was designed to have an external diameter of 60mm, an internal diameter of 56 mm and a length of 1.3m. This had a direct impact on the propellant since the propellant casing is required to have a maximum outer diameter of 56mm in order to fit in the airframe.

These design requirements, among others, shown in Table I, were the objectives to be met during the design process.

TABLE I
DESIGN REQUIREMENTS

Name	Apogee (m)
Apogee	500 m
Propellant Composition	KNSB
Propellant Type	Solid
Propellant Casing Material	Aluminium
Propellant Casing Diameter	56 mm
Approximate Rocket Mass	3.5 kg

The design process was done sequentially beginning with the casing and ending with the nozzle. During the design process, pressure and temperature were checked to ensure the casing did not melt at elevated temperatures or give in under pressure.

Iterative designs for the solid rocket motor were done and the final design is as shown in Fig. 1 and Fig. 2.

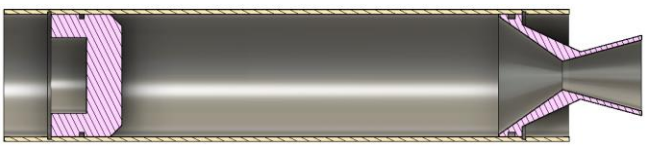

Fig. 1 Sectional view of designed motor

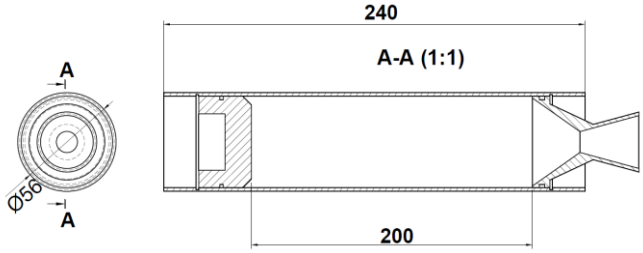

Fig. 2 Assembled motor drawing

The design of the individual components is broken down into the following sections.

A. Casing Design

This process began with the determination of the casing material, dimensions and length that could sustain the combustion temperatures and pressure. Considerations for the casing material included the weight, melting point, yield strength and ultimate tensile strength.

Since the outer diameter of the casing was limited to 56 mm, a suitable wall thickness had to be determined to achieve a balance between strength and minimising weight. The casing is exposed to high pressures of about 2 MPa that has to be contained within the casing. 6063, 7075 Aluminium and AISI 1025 steel were the materials considered for the casing.

7075 Aluminium was initially chosen among these due to its high strength (yield strength: 455 MPa, ultimate strength: 531 MPa), which is almost as strong as mild steel. The advantage of 7075 Aluminium is that it is lightweight and easy to machine, while its drawback is the low melting point of approximately 483°C. This drawback was easily overcome by adding an insulation layer, however, the solution was not long lasting since the casing melted severally. The eventual solution was to use a steel tube, a solution that was to be implemented in the next fabrication stage.

With a 2 mm wall thickness, the design pressure was found to be 13 MPa with a burst pressure of 42 MPa. A safety factor of 2.5 was used for the design pressure and 3.26 for the burst pressure. These values were found according to equation 1.

$$P_D = 2\frac{t \times F_{ty}}{D_o \times S_D} \quad (1)$$

Where P_D is the design pressure, t is the wall thickness, F_{ty} is the yield strength, D_o is the outer wall diameter and S_D is the safety factor.

This design pressure was much higher than what could be generated by the solid propellant motor; a further decrease in the casing thickness would introduce difficulty in fabrication.

The final design of the casing was as shown in Fig. 3.

A casing length of 240 mm was used to contain 2 fuel segments of propellant with 100 mm length. A 1 mm deep groove was also designed to incorporate a snap ring (circlip) that would be used as a retainer for the nozzle and bulkhead. The advantage of a snap ring is that it ensures no drilled and threaded holes are added to the casing that would compromise the structural integrity of the casing.

Snap rings also have the advantage of easy installation over bolts that need to be aligned and that no holes would need to be drilled into both the nozzle and the bulkhead.

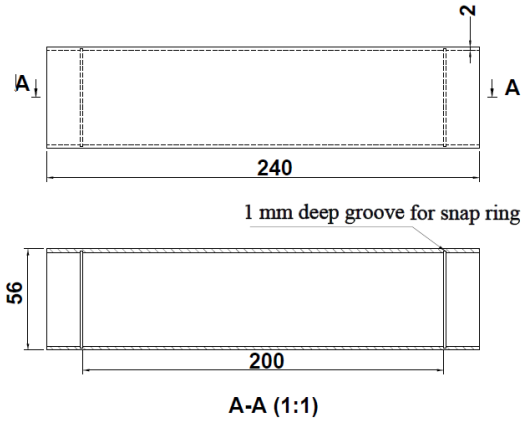

Fig. 3. Casing design

B. Solid Rocket Propellant Design

For the *N-1* rocket [13], previously undertaken by the Nakuja project, KNSU (Potassium Nitrate and Sucrose) was used as its propellant. Despite the high thrust values this fuel provides, it has the effect of exceedingly high pressures that are potentially dangerous. The N-2 rocket uses a KNSB (Potassium Nitrate and Sorbitol) propellant that has slightly lower pressures and lower thrust values generated. However, it is much safer and easier to cast.

The Solid Propellant, KNSB, was designed in conjunction with the simulation process as most of the design parameters involved chemical reactions. The propellant was composed of potassium nitrate (oxidiser), sorbitol (fuel), and red iron (III) oxide (burn rate modifier).

A stoichiometric ratio of the fuel to the oxidiser is described as 37:63 [14], however, from testing, a modification to this ratio proved that a ratio of 34:66 yielded better results in terms of the thrust generated and in reducing the burn time. 5 percent of the burn rate modifier was used to enhance the burn rate and get it as close to the simulation values as possible.

From the volume of the casing chamber and the density of KNSB (1.841 g/cm^3) it was found that a total mass of 600 g of propellant would be required to fill the casing chamber. The ratios of the constituents were computed from the total mass of the fuel, and an additional 20% of each constituent was added to account for losses.

The required masses of the individual components were as shown in Table II.

TABLE II
FUEL COMPOSITION

Constituent	Mass
Potassium nitrate	964 g
Sorbitol	672 g
Iron III oxide	14.4 g

C. Bulkhead Design

The purpose of the bulkhead is to act as an airtight seal for the casing to ensure all exhaust gas is released from the nozzle. The bulkhead is designed in such a manner that ensures in the event of any failure in the system, it will be released, protecting both the casing and the nozzle as they are more difficult to fabricate.

The casing was equipped with an O-ring that serves as a pressure seal. It was retained using the same snap rings used for retaining the nozzle. The bulkhead was also made of 7075 Aluminium alloy that has the same properties as the casing. 10 mm thickness was used and an outer diameter of 52 mm. It was also designed to have a 2 mm deep groove for installation of the O-ring. This design assumes a force fit of the bulkhead into the casing to keep it airtight and prevent any pressure leaks.

The initial design of the bulkhead was to be retained using bolts. This however had the effect of an increased mass and a compromise in the structural integrity of the casing. The final design of the bulkhead is shown in Fig. 4.

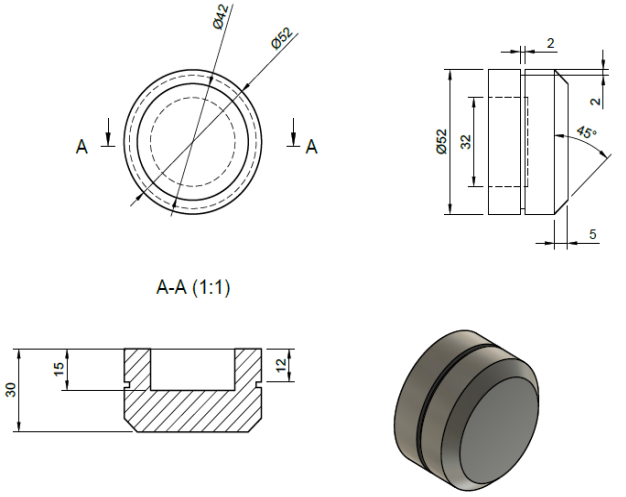

Fig. 4. Bulkhead design

D. Nozzle Design

The nozzle was designed with the goal of ensuring that maximum thrust was obtained from the developed propellant. A significant parameter in the design of nozzles is the expansion ratio **ε**, which is defined as the ratio of the nozzle exit area, A_e to that of the nozzle throat area, A_t given as in equation (2) [15].

$$\varepsilon = \frac{A_e}{A_t} \qquad (2)$$

The nozzle's aim is to convert the high pressure and temperatures of the combustion chamber into kinetic energy thus maximising exit velocity hence improving the thrust of the motor [16].

Two types of nozzles were evaluated by simulation before fabrication to ensure that optimum performance of the motor was obtained. Great care was taken in the design of the nozzle since it is the most difficult part to fabricate.

Geometrically, the difference between the two nozzles is that one had an entry diameter equal to the exit diameter, while the other had an exit diameter which ensured an optimum expansion ratio. An optimum de laval nozzle is shown in Fig. 5. The design of the nozzle began with a determination of the throat diameter. The throat diameter was determined from the maximum pressure that could be sustained by the casing.

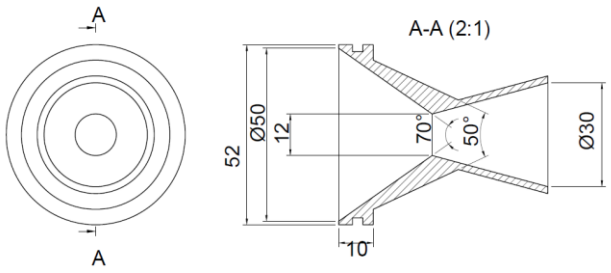

All dimensions in mm

Fig. 5. First nozzle design

To determine the value, the tool SRM.xls was used to get the appropriate throat diameter[17]. The throat diameter of the nozzle is obtained to ensure that the pressure does not exceed the preset value in order to prevent any failures of the casing. Using the SRM.xls tool, the throat diameter was found as 11.6 mm. Due to a limitation in the available tools, this was rounded up to 12 mm since a drill bit of this diameter is readily available. The nozzle's entry diameter was limited to that of the casing's inner diameter, i.e., 52 mm. However, due to the difficulty in obtaining a sharp edge, a short flat edge was added and an entry diameter of 50 mm was used instead.

For de laval nozzles, the recommended converging angle is between 30 and 50 degrees [5], a value of 35 degrees is initially selected for the specific nozzle to be used in this propellant. Variation of the converging and diverging angle within these limits has no significant effect in the propellant's performance [18].

The expansion ratio of the optimised nozzle was found to be 4.181, found from equation 3 below.

$$\frac{A}{A_e} = \left(\frac{k+1}{k-1}\right)^{\frac{1}{k-1}} \left(\frac{P_e}{P_o}\right)^{\frac{1}{k}} \sqrt{\left(\frac{k+1}{k-1}\right)\left[1-\left(\frac{P_e}{P_o}\right)^{\frac{k-1}{k}}\right]} \qquad (3)$$

Where:

K *is* the constant, given as 1.15
P_e is the pressure at nozzle exit plane, atmospheres
P_o is the stagnation pressure (chamber pressure)

The exit diameter was thus found from the expansion ratio as 28.63 mm using equation 3. However, due to challenges in fabrication, this value was rounded up to 30 mm to allow for easier fabrication.

Design for the full-length nozzle was straightforward since for the full-length nozzle the exit diameter is equal to the entry

diameter, giving an expansion ratio of 17.361. A throat of 12 mm was also used for this nozzle.

This design is shown in Fig. 6. Both nozzle designs were analysed using the finite element analysis (FEA) methods to numerically quantify the performance of each nozzle before the final selection was done. The results of this analysis, as shown in the simulation section, proved that the optimum nozzle was best suited for the developed motor.

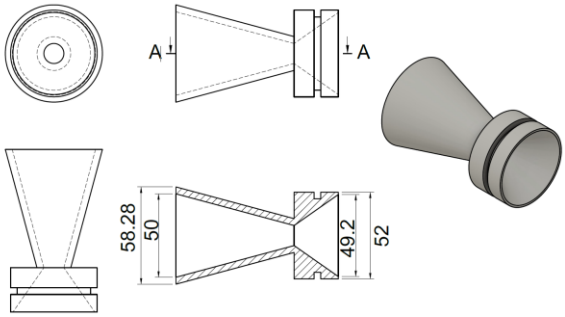

Fig. 6 Full length nozzle

This initial nozzle was designed to be fabricated from 7075 aluminium due to its availability and ease of fabrication. During the testing of this nozzle, the nozzle melted in the second test due to the low melting point of 7075 aluminium. This challenge necessitated the change of material from 7075 aluminium to AISI 1018 steel. The alternate nozzle shown in Fig. 3 was then fabricated from 1018 steel as discussed in the fabrication section.

III. SIMULATION

The main goal of the simulation process was to evaluate the design parameters and to validate the designs prior to fabrication. Simulation also played an important role in fabrication since it guided the choices of the fabrication methods and processes.

The processes of simulation, design, fabrication and testing were done concurrently with modifications being done in each step in order to enhance the propellant's output.

Simulations were done on different parts of the design as listed below.

1. Nozzle
2. Propellant
3. Entire rocket

Ansys Fluent was used to perform simulation of the nozzle that was modelled on Fusion 360. OpenRocket and OpenMotor were used to perform simulations on the propellant and the rocket respectively. Effect of the nozzle on the propellant's performance was further quantified using OpenMotor software.

The simulation process is discussed in detail as follows.

1. Nozzle simulation

The effect of the nozzle was simulated in two steps, first was using OpenMotor to evaluate the impact of the nozzle on the generated thrust and finally computational fluid dynamics to evaluate the effect of flow through the nozzle.

After the setup of the propellant in OpenMotor, the nozzle dimensions were input into the simulation parameters. The values as placed in the software are indicated in Table III.

TABLE III
NOZZLE PARAMETERS

Parameter	Value
Throat diameter	12mm
Exit diameter	30 mm
Entry diameter	50 mm
Convergence half angle	30°
Divergence half angle	15°

A simulation of the performance of the propellant with the two nozzles was done and the results of the simulation were as shown in Table IV.

TABLE IV
PROPELLANT PARAMETERS

Parameter	Nozzle 1	Nozzle 2
Designation	I263	J342
Impulse	435.02 Ns	657.55 Ns
Delivered Isp	90.91 s	119.56 s
Burn time	1.62 s	1.89s
Propellant mass	0.56 kg	0.56 kg
Peak pressure	2.29 MPa	2.29 MPa

From the results, it is clear that the optimum nozzle gives a better performing nozzle as compared to the full-length nozzle. Further investigation of the two nozzles is done as illustrated in the subsequent sections.

Nozzle CFD analysis

The nozzle was subjected to finite element analysis to establish the effect of flow through it. Ansys Fluent was used for this purpose. Both the optimum nozzle and the full-length nozzle were subjected to FEA in an attempt to select the most suitable nozzle for the motor.

The dimensions for both the full-length nozzle and the optimised nozzle are given in the design section.

The simulation process began with a setup of the geometry of the nozzle in the inbuilt modelling software, Design Modeller. The geometry setup was done in conjunction with a setup of the flow domain to be analysed.

After the geometry setup, a mesh of the area to be analysed was generated and the inlet and outlet indicated. Quadrilateral meshes were used in this step since they have an added accuracy over the triangular meshes. An illustration of the meshed profile is shown in Fig. 7.

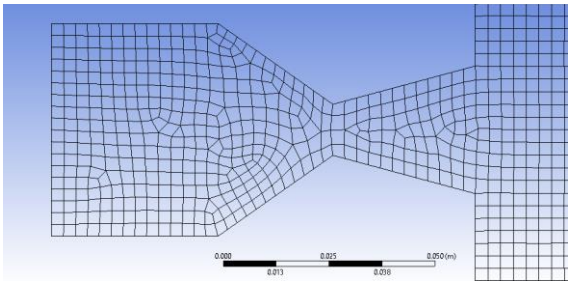

Fig. 7. Mesh on the nozzle cross section

The simulation setup was done for a static pressure-based simulation using an SST k-omega solver. The simulation setup parameters are shown in Table V.

TABLE V
SIMULATION PARAMETERS

Property	Value
Pressure Inlet	2268000 Pa
Inlet Temperature	1200 K
Inlet Velocity	17.1 m/s
Viscosity	Sutherland
Thermal Conductivity	0.0242 (W/m.K)

The simulation was done for 4500 iterations before it converged and the results analysed. The results of the simulation are plotted as shown in Fig. 8.

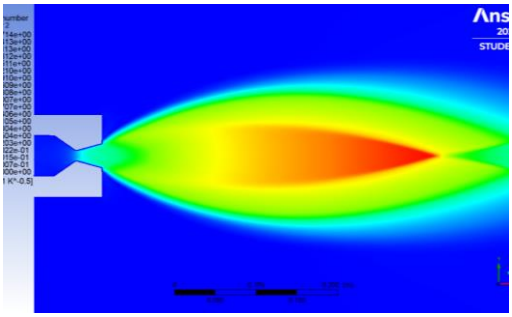

Fig. 8 Velocity distribution for nozzle 1

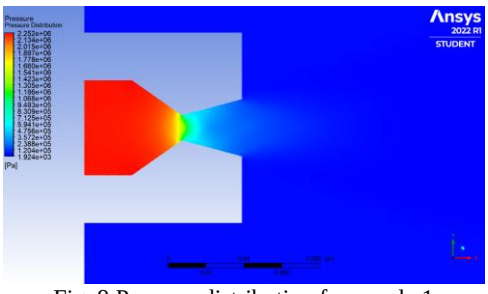

Fig. 9 Pressure distribution for nozzle 1

From the simulation, it is seen that maximum pressure is experienced at the inlet. It is also noted that at the inlet of the nozzle, the velocity of the exhaust gases is low (17.1 m/s).

However, at the nozzle diverging section, pressure of the exit gases begins to decrease from 2.252 MPa to near ambient values (1.924 KPa). On the other hand, the velocity of the gases is greatly increased, to a maximum value of Mach 5.

The full-length nozzle subjected to the same inputs and boundary conditions yields the results shown in Fig. 10.

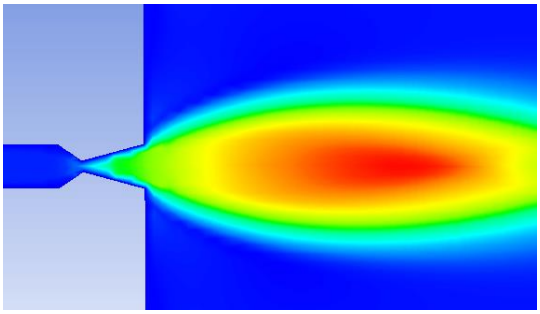

Fig. 10. Full length nozzle velocity analysis

From the simulation, it is noted that the velocity of the gases at the exit is 1413 m/s (Mach 4), while that at the inlet is 17.2 m/s. Despite the pressure drop in both nozzles being the same, the exit velocity of the gases at the exit of both nozzles shows that the optimum nozzle offers a slightly better advantage in terms of the performance of the propellant it is connected to.

The first nozzle further has the advantage that it consumes less space and weight, thus keeping the rocket mass at a reasonable minimum.

2. Propellant performance simulation

The KNSB propellant was simulated using OpenMotor. This was used to quantify the rocket's thrust from the chemical properties of the propellant. A simulation of the rocket's thrust with and without the nozzle was done. Two types of nozzles were investigated using this fuel, the optimum nozzle and the full-length nozzle. The results of these simulations are presented in the nozzle simulation section.

The propellant parameters used for this simulation are as shown in Table VI.

TABLE VI
PROPELLANT PARAMETERS

Parameter	Value
Length	200 mm
Core diameter	19 mm
Outer diameter	50 mm
Inhibited ends	Both

It is noted that the highest thrust generated when the first nozzle is used. This data influenced the selection of the first nozzle for the N-2 rocket motor. According to the generated thrust values, the designed rocket motor was classified as shown in Table VI above.

3. Rocket simulation

The impact of the designed J-class rocket motor to the entire rocket was simulated by using OpenRocket. Data generated from the simulation done on OpenMotor was exported as a single file and this included in the rocket designed in the OpenRocket software.

The goal of this simulation is to determine the maximum apogee that can be achieved by the rocket once equipped with

the solid rocket motor. The rocket designed on OpenRocket included the parachute, the nose cone, the fuselage, the electronics and the propellant. This is shown in Fig. 11.

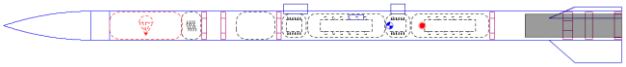

Fig. 11. Rocket Setup

A simulation of the performance of the rocket with the propellant was done on the software. The rocket was set up, equipped with the simulated motor and the results are shown in Table VII.

TABLE VII
SIMULATED ROCKET PERFORMANCE

Parameter	Value
Apogee	564 m
Time to Apogee	11.2 s
Maximum Velocity	110 m/s
Velocity at deploy	0.997 m/s

The results, as shown in Table VII, show an apogee of 564m which indicates that the desired objectives of the rocket could be achieved.

The next step in this process is to begin the fabrication of the different parts while following the design parameters. Testing of the fabricated parts determined whether the design had to be modified or remained as is.

IV. FABRICATION

Fabrication of the different parts of the solid propellant motor was locally done: the casing, bulkhead, nozzle, propellant, and igniters.

After fabrication, the components were assembled and the propellant grains packed inside the casing. This assembly is shown in Fig. 12.

Fig. 12 . Motor assembly

The fabrication of the individual components are discussed in detail as follows.

1. *Casing*

The casing is required to have the profile of a hollow cylinder / tube with a thickness of 2 mm and inner diameter 52 mm. The ideal option would be to use a drawn aluminium tubing with this profile and do minor modifications to get it to the dimensions required. However, this was not possible due to the expenses required to perform a custom extrusion since an already extruded profile was not available.

The process began with the acquisition of an aluminium rod with a diameter of 65 mm that was turned on the lathe to the required diameter (56 mm). This was followed by progressive drilling operations from 12 mm all the way to 50 mm and finally boring of the drilled hole to 52 mm diameter. The final operation was to machine the groove required to hold the s to be used as retainers for the bulkhead and nozzle.

The fabricated casing is shown in the figure below.

2. *Bulkhead*

The bulkhead was fabricated from a 65 mm diameter aluminium rod. The process involved turning, grooving, chamfering and facing. The final operation involved filing of the bulkhead to ensure it fits perfectly into the casing.

An image of the fabricated bulkhead is shown in Fig. 13.

Fig. 13. Fabricated bulkhead

The bulkhead was fitted into the casing and retained using a snap-ring as shown in Fig. 14 below. Prior to fitting, an O-ring was inserted into the groove to provide a pressure seal that ensures all pressure is retained within the casing and is only released through the nozzle.

Fig. 14. Bulkhead fitted into casing

3. *Nozzle*

Fabrication of the nozzle was the most tedious and lengthy process. The main challenge being the fabrication of the convergent and divergent tapers. Fabrication of the nozzle was done from a 1018 mild steel rod of 70 mm external diameter. The large

diameter rod was used since it was very readily available and no procurement was needed.

The fabrication process began with turning the rod to 52 mm, followed by drilling of the nozzle's throat (12 mm) ,then machining of the internal taper of the nozzle's convergent side and finally machining of the O-ring groove.

The workpiece was then removed and re-clamped to enable fabrication of the surfaces on the opposite end. The divergent section of the nozzle was machined, both the inner and outer surfaces, by taper turning. An allowance for the surface's mating with the internal circlip was left.

The fabricated nozzles are shown in Fig. 15.

Fig. 15. Fabricated nozzle

The fabricated nozzle was fitted into the fabricated casing, on the end opposite to that of the bulkhead and retained using snap rings. This assembly is shown in Fig. 16.

Fig. 16. Nozzle - casing assembly

4. *Casting Tools*

Casting tools were fabricated to aid in the casting process of the fuel. They include the casing responsible for giving shape to the fuel and a coring rod for setting the required core diameter of the fuel grains. The casting tools were made of PVC tubing secured on a piece of plywood using hot glue and fitted with parchment paper that served as an insulation. This setup is shown in Fig. 17.

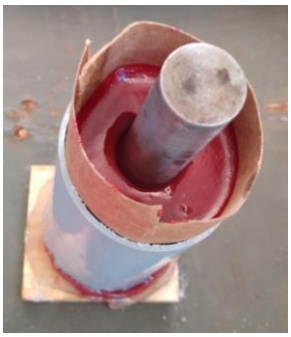

Fig. 17. Casting tools with fuel

5. *Propellant*

To achieve a homogenous fuel-oxidiser mixture, the casting process was preferred. This involved heating of the propellant constituents to the melting point of the fuel and adding the oxidiser. This is normally done for powdered constituents. However, the sorbitol available was found in solution form that contained 70% by mass of water. For this to be used in the casting process,the liquid sorbitol had to be heated to evaporate all water content before adding the oxidiser.

Heating of the sorbitol solution was done without monitoring the temperatures since sorbitol exhibits no effects of caramelization due to overheating [4]. The process was monitored visually while observing the point at which evaporation ended completely.

After this, casting was ready to be performed, at the casting temperature (110 °C-135 °C) [2]. The heated sorbitol was allowed to cool while its temperature was being monitored by a thermal infrared thermometer.

At 110 °C, ground and sifted potassium nitrate was added to the sorbitol and the temperature maintained within the range of 110 °C to 135 °C during the whole process. The final step in the casting process was to add 1% of red iron III oxide that gave the casting a red colour. An image of the molten propellant is shown in Fig. 18.

Fig. 18. Propellant casting

The next step was to pour the molten propellant, now in the form of a slurry, into the casting tools to allow for it to cure. The propellant was designed to have a BATES grain, which was also easily achieved using the available casting tools. The propellant curing in progress is shown in Fig. 19.

Fig. 19. Propellant curing

After curing, which takes roughly 24 hours, the propellant is extracted from the casting tools and is ready to be ignited. The fuel, having been cured, still needs to be mounted inside the casing in order to contain all the pressure generated and use a nozzle to enhance the motor performance.

The fuel grain is placed in the casing with an insulating material between it and the casing as shown in Fig. 20.

Fig. 20. Cured propellant mounted inside casing

Two grains of the cured fuel are then inserted into the casing and the casing was sealed on either ends by the nozzle and the bulkhead.

6. *Igniters*

The main purpose of the igniters was to ensure the fuel is appropriately ignited upon transmission of the ignition command. A chemical igniter was made for this purpose.

The igniters were made of a mixture of potassium nitrate (KNO_3) and charcoal. The two were ground together in the ratio 80:20, potassium nitrate to charcoal respectively. After preparation, the igniter powder is packed in a paper straw and an electrical wire placed inside the straw. A short length, 5 mm, of nichrome wire is placed inside the powder to supply the required heat to ignite the entire powder.

Despite several failures during initial testing, the igniter proved to be a reliable method of igniting the fuel.

V. STATIC TESTING

With all the components fabricated, the next step in the development of the propellant was to perform testing in order to get enough data to validate the designs. Testing of the propellant made use of a fabricated test stand, not discussed here, that had the task of collecting the thrust generated from the propellant. Data was collected from the test stand and analysed in comparison to the simulated values of thrust.

A total of 4 static tests were done, with improvements being done in each stage in order to achieve the desired outcome. Breakthrough was made in the 3rd static test, where the thrust values became more steady and closer to the simulated values. The results of the four conducted static tests done are presented as follows.

A. Static Test 1 & 2

During the initial stages of fuel preparation, the fuel was prepared without blending of potassium nitrate and heating of the sorbitol solution was not done thoroughly. This had the effect of leaving too much residual moisture in the fuel and thus the burn time was prolonged.

In the first two static tests, an average burn time of 34 seconds was obtained which was an indication of a very slow burn rate. There was also very little thrust generated, 24 Newtons and 51 Newtons, as a result of the slow burn rate.

An inspection of the fuel after the static test showed too much residue within the casing after the burn, an undesirable effect. This is shown in Fig. 21.

Fig. 21. Combustion aftermath

It was also noted that there was a slight erosion of the nozzle.

B. Static Test 3

Modification of the fuel preparation was done, which included the grinding of Potassium Nitrate into very fine particles and thorough heating of sorbitol solution to ensure all water is vapourized was done.

More of the burn rate modifier was used (6%) and the oxidiser to fuel ratio changed to 67:33.

The Static Test generated a peak thrust of 160 Newtons, a value that neared the simulated thrust (206 N). A much shorter burn time was also achieved, 3.2 s.

However, the static test was a partial failure since the nozzle melted. This is shown in Fig. 22.

Fig. 22. Melted nozzle

A further inspection of the aftermath showed that there was almost no residue left, beside the insulation layer.

C. Static Test 4

A new nozzle was fabricated out of mild steel and the fuel preparation parameters retained as in Static Test 3. The static test was a success, yielding a peak thrust of 182 Newtons, which exceeded the simulated values.

A comparison of the results of the above mentioned static test is summarised in Fig. 23.

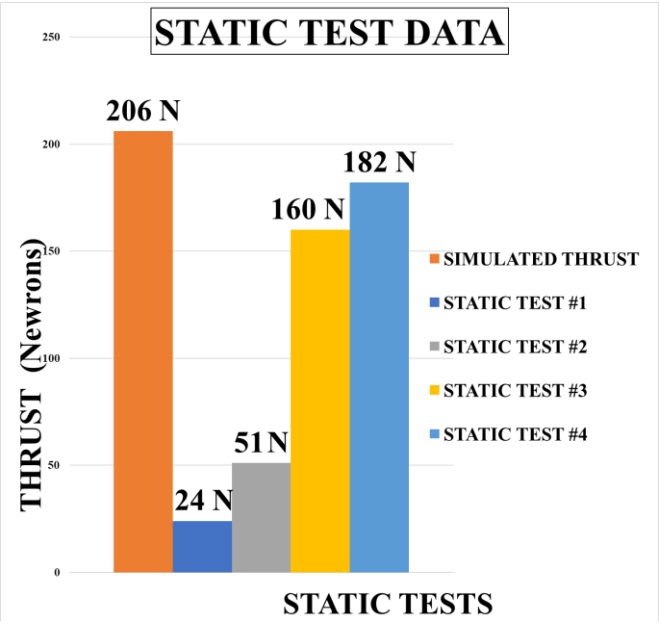

Fig. 23. Static test summary

VI. DISCUSSION

Development of the solid propellant motor is influenced by a number of factors, i.e., the nozzle, the casing, and the fuel preparation.

The nozzle, as seen from the simulation, had a significant impact on the thrust achievable by the motor, with the full and optimum nozzles being investigated.

An aluminium nozzle was fabricated initially and used for the first 2 static tests before it melted during the static test. The melting of this nozzle was attributed to aluminium 7075`s relatively low melting point of 643 °Cc

The steel nozzle developed had a much higher melting point of 1200 °C that could withstand the temperatures of the burning fuel.

From the static tests performed, it was noted that several factors in the preparation of the fuel (casting) had an effect on the eventual thrust development. These were,

- The oxidiser (Potassium Nitrate) grain size
- The oxidiser to fuel ratio
- The burn modifier (quantity)
- Amount of moisture present

It was found that very fine grains of the oxidiser (blended and sifted) produced a higher thrust since it ensured that the oxidiser fuel mixture was homogenous and decreased the burn time which gave a higher thrust. It was also noted that despite the recommended oxidiser to fuel ratio of 65:35 [4], a ratio of 67:33 gave an improved motor performance. The recommended quantity of the burn modifier (Red iron oxide) was 1% of the total propellant mass. It was discovered however that an increased quantity, 1.5%, yielded a faster burn rate as compared to the initial 1%. It also had the effect of ensuring minimal burn residue. This is because red iron oxide acts as a catalyst and speeds up the reaction and thus increasing the rate at which the exhaust gases are liberated.

The amount of moisture in the propellant, when using sorbitol solution, has a great impact on the quality of the developed propellant. When not properly heated to ensure all water is evaporated, the propellant quality drastically reduces. The burn time is greatly increased and the propellant takes exceedingly long to cure.

VII. CONCLUSION

A high-powered propulsion system for the Nakuja-2 rocket was successfully designed, simulated, and developed with an average thrust of 151.7 Newtons which is above the threshold of 80 Newtons. The ratio of oxidizer to fuel, 66:34, was found to produce more thrust than the stoichiometric ratio, 65:35. This is evidenced by the fourth static test where the motor performance exceeded the simulated results.

It was noted that the properties of Aluminium made it an appropriate material for the use of the casing. It is light and is able to handle the high pressure and temperature of combustion. It is however not suitable for the nozzle as it has a low melting point. Steel is preferred for this application. The high powered

propulsion system was able to propel a model rocket to an apogee of 280m.

An optimum nozzle design was used and the developed solid propellant motor was able to generate an average thrust of 151.7 Newtons. It is recommended to have specially designed casting tools that enable curing under pressure and a consistent grain size.

Due to the significance of the nozzle in the propellant, it is also recommended to have advanced tools for the fabrication of the nozzle, such as the use of Computer Numerically Controlled machines or using Powder Metallurgical methods for nozzle fabrication.

ACKNOWLEDGEMENT

We would like to acknowledge the continued help of the Africa-Ai-Japan Project (JICA) who have funded this research.

REFERENCES

[1] B. Wang, "Current Technologies And Challenges Of Applying Fuel Cell Hybrid Propulsion Systems In Unmanned Aerial Vehicles." Progress In Aerospace Sciences, Vol. 116, P. 100620, 2020, Doi: 10.1016/J.Paerosci.2020.100620.

[2] A. Okninski, "Solid Rocket Propulsion Technology For De-Orbiting Spacecraft." Chinese Journal Of Aeronautics, Vol. 35, No. 3, Pp. 128-154, 2022, Doi: 10.1016/J.Cja.2021.07.038.

[3] L. T. Deluca, M. A. Bohn, V. Gettwert, V. Weiser, And C. Tagliabue, "Innovative Solid Rocket Propellant Formulations For Space Propulsion." Energetic Materials Research, Applications, And New Technologies, Pp. 1-24, 2018, Doi: 10.4018/978-1-5225-2903-3.Ch001.

[4] M. Abousabae, R. S. Amano, And C. Casper, "Investigation Of Liquid Droplet Flow Behavior In A Vertical Nozzle Chamber." Journal Of Energy Resources Technology, Vol. 143, No. 5, 2021, Doi: 10.1115/1.4049465.

[5] Z. Li, N. Wang, B. Shi, S. Li, And R. Yang, "Effects Of Particle Size On Two-Phase Flow Loss In Aluminized Solid Rocket Motors." Acta Astronautica, Vol. 159, Pp. 33-40, 2019, Doi: 10.1016/J.Actaastro.2019.03.022.

[6] T. Ecker, S. Karl, And K. Hannemann, "Modeling Of Aluminum Particle Combustion In Solid Rocket Combustion Chambers." 53rd Aiaa/Sae/Asee Joint Propulsion Conference,2017,Doi:10.2514/6.2017-4781.

[7] D. Greatrix, "Numerical Evaluation Of The Use Of Aluminum Particles For Enhancing Solid Rocket Motor Combustion Stability." 2021, Doi: 10.32920/14640180.V1.

[8] K. E. Uhlenhake, "On The Use Of Fluorine-containing Nano aluminium Composite Particles To Tailor Composite Solid Rocket Propellants." Propellants, Explosives, Pyrotechnics, 2022, Doi: 10.1002/Prep.202100370.

[9] L. T. Deluca, "Overview Of Al-Based Nanoenergetic Ingredients For Solid Rocket Propulsion." Defence Technology, Vol. 14, No. 5, Pp. 357-365, 2018, Doi: 10.1016/J.Dt.2018.06.005.

[10] M. Yu, Z. Zhu, H.-P. Li, And Q.-L. Yan, "Advanced Preparation And Processing Techniques For High Energy Fuel Alh3." Chemical Engineering Journal, Vol. 421, P. 129753, 2021, Doi: 10.1016/J.Cej.2021.129753.

[11] S. Pradhan, V. Kedia, And P. Kour, "Review On Different Materials And Their Characterization As Rocket Propellant." Materials Today: Proceedings, Vol. 33, Pp. 5269-5272, 2020, Doi: 10.1016/J.Matpr.2020.02.960.

[12] T. Aarant, "The Development Of A Powder-Filled, Abs Matrix For Use As Fuel In A Hybrid Rocket Motor." Aiaa Propulsion And Energy 2019 Forum, 2019, Doi: 10.2514/6.2019-4417.

[13] F. W. Gateru, S. K. Oina, J. Mboya, I. Kibandi, B. Owiti, and S. Aoki, "Development of Solid Propellant Motor for Low Altitude Model Rockets," p. 8, 2021.

[14] G. P. Sutton and O. Biblarz, "Rocket Propulsion Elements," p. 792.

[15] R. Hiers and R. Knapke, *The Optimum Rocket Nozzle Expansion Ratio: An Air – to – Air Missile Demonstration*. 2019. doi: 10.2514/6.2019-4382.

[16] S. W. Graves, J. P. Nolan, J. H. Jett, J. C. Martin, and L. A. Sklar, "Nozzle design parameters and their effects on rapid sample delivery in flow cytometry," *Cytometry*, vol. 47, no. 2, pp. 127–137, 2002, doi: 10.1002/cyto.10056.

[17] O. Durif, "Design of de Laval nozzles for gas-phase molecular studies in uniform supersonic flow," *Phys. Fluids*, vol. 34, p. 013605, Jan. 2022, doi: 10.1063/5.0060362.

[18] B. Lin, H. Pan, L. Shi, and J. Ye, "Effect of Primary Rocket Jet on Thermodynamic Cycle of RBCC in Ejector Mode," *Int. J. Turbo Jet-Engines*, vol. 37, Jan. 2017, doi: 10.1515/tjj-2017-0013.